Plastic Deformation of Polypropylene in Relation to Crystalline Structure

ROLAND SEGUELA,[1] ERIC STANIEK,[1] BERTRAND ESCAIG,[1] BERTRAND FILLON[2]

[1] Laboratoire Structure et Propriétés de l'Etat Solide, URA CNRS 234, Université des Sciences et Technologies de Lille, Bât. C6, 59655 Villeneuve d'Ascq Cedex, France

[2] Centre de Recherche de Voreppe, Pechiney Co., 38340 Voreppe, France

Received 10 September 1997; accepted 19 August 1998

ABSTRACT: The tensile drawing behavior of quenched and annealed films of isotactic polypropylene is investigated as a function of draw temperature and strain rate. A strain-induced structural change from the smectic to the monoclinic form is observed for the quenched films. A kinetic interpretation is proposed for the phenomenon. Data of thermal activation volume at the yield point indicate two regimes of plastic flow for the quenched sample, between 25 and 60°C, but only one regime for the annealed sample. Homogeneous and heterogeneous crystal slip processes are proposed to account for these regimes in relation to the nucleation and propagation of screw dislocations. The basic mechanism of molecular motion in the polypropylene crystal is suggested to be a wormlike motion of conformational defects along the 3/1 helix chains that allows a 120° rotation and a *c*/3 translation. The occurrence of the smectic form as a transitory state in the deformation pathway is discussed in terms of plasticity defect generation. © 1999 John Wiley & Sons, Inc. J Appl Polym Sci 71: 1873–1885, 1999

Key words: polypropylene; smectic form; monoclinic form; plasticity; dislocations; crystal slip; mechanical relaxation

INTRODUCTION

The continuing search of mechanical improvement of polypropylene-based composites and molded parts, as well as the increasing development of biaxially oriented polypropylene films in the packaging market, have aroused a renewed interest for the mechanisms of plasticity of this material. The investigations reported in the early 1970s by Peterlin and coworkers[1–3] have demonstrated the major contribution of the crystalline phase in the tensile deformation process of polypropylene above room temperature. Since then, there has been a number of articles dealing with the orientational behavior of the chains either as a function of the deformation conditions or in relation to the use properties of the drawn materials.[4–7] More recent studies have shown that crystallographic slip along planes parallel to the chain axis is more probably the main active process of plasticity of polypropylene for various deformation modes, namely, tensile drawing,[8] simple shear,[8,9] and compressive testing.[10,11] This turns out to be a general behavior of semicrystalline polymers, as notably shown for polyethylene[12–14] and polyamides.[15,16] However, the elementary mechanisms of crystal plasticity in

---

Present address: Eric Staniek, Département Matériaux et Technologies Nouvelles, Institut Catholique des Arts et Métiers, 6 rue Auber, 59046 Lille, France.
Present address: Bertrand Fillon, American National Can, Neenah Technical Center, 2301 Industrial Drive, P.O. Box 702, Neenah, Wisconsin 54957-0702.

Correspondence to: R. Seguela.

Contract grant sponsor: Pechiney Co.

Journal of Applied Polymer Science, Vol. 71, 1873–1885 (1999)
© 1999 John Wiley & Sons, Inc.
CCC 0021-8995/99/111873-13

polypropylene are certainly more complicated than in the case of polyethylene, which is its unsubstituted chemical homolog, because of more complex chain conformation and crystal structure.

The present work deals with the tensile drawing of polypropylene in relation to the initial organization of the crystalline phase of quenched and annealed films. Particular effort is devoted to the understanding of elementary events of plasticity in terms of the molecular motion.

EXPERIMENTAL

The commercial-grade isotactic polypropylene (PP) under investigation has weight- and number-average molar weights $M_w = 257{,}000$ and $M_n = 52{,}000$. Films 100 μm thick were cast at 230°C from a T-die extruder and subsequently quenched on a chill roll at 30°C. Film pieces have been annealed at 140°C for 1 h to improve crystal perfectness. The quenched and annealed films are labelled QPP and APP, respectively.

Thermal analysis has been carried out on a DSC-7 Delta apparatus from Perkin–Elmer, at a scanning rate of 10°/min. The sample weight was about 5 mg. The temperature and heat flow scales were calibrated using the melting peaks of high purity indium and zinc samples.

Wide-angle X-ray scattering (WAXS) patterns of drawn samples have been recorded on a flat film camera. The Ni-filtered X-ray beam was generated by a Siemens tube operated at 40 kV and 25 mA. Measurements of scattering intensity profiles from isotropic, as well as oriented, samples have been performed on a diffractometer equipped with a bent quartz crystal monochromator and using a curved position-sensitive counter INEL CPS120 of 225 mm radius. Samples consisting of sixfold wrapped strips were held into Lindemann glass tubes in order to increase the scattered intensity.

The viscoelastic behavior of the films has been studied in tensile mode on a Rheometrix RSA II apparatus at 1 Hz. The sample dimensions were 25 and 5 mm in gauge length and width, respectively.

Mechanical experiments have been conducted on an Instron tensile testing machine at various draw temperatures (T_d) in the range 5–60°C and various crosshead speeds (CHS) in the range 0.1–800 mm min. The dumbbell-shaped samples having 60 and 8 mm gauge length and width, respectively, were cut from the films with a cutting die.

The nominal stress or engineering stress σ_N is defined as the ratio of the draw force to the initial cross section. The nominal strain or engineering strain ε_N is the ratio of the deformed sample length to its initial gauge length. It is to be noticed that the nominal strain has no physical meaning during the occurrence of a plastic instability, that is, necking. However, when deformation is homogeneous, that is, prior to the yield point and beyond the propagation of the neck over the whole length of the sample, the nominal strain is the actual strain. The true yield stress is thus given by $\sigma_Y = \sigma(1 + \varepsilon_Y)$, where ε_Y is the true strain at the yield point. The standard deviation of the data is about 3%. The initial strain rate $\dot{\varepsilon}$ is assessed from the ratio of the crosshead speed to the initial gauge length of the sample.

The thermal activation of the plastic flow has been studied through activation volume measurements at the yield point as a function of draw temperature and strain rate. Using thermal activation analysis, the apparent activation volume can be derived from the yield stress dependence on strain rate (see the Activation Volume Determination and Signification Section in the Appendix). For the sake of comparison, activation volume determinations have also been achieved as a function of strain rate from stress relaxation measurements at the tensile yield point, following a procedure previously described[17] in the case of compressive plastic flow of bulk PP below the glass temperature transition (see the Stress Relaxation Measurements Section in the Appendix).

Great care must be taken when giving to the activation volume data the physical meaning of the critical size of the activated defect of plasticity, that is, the volume of matter involved in the elementary shear event. As a matter of fact, this only applies to the true activation volume, which is a part of the apparent activation volume.[18] However, it is shown in the Appendix that, in the present study, the former one represents more than 80% of the latter one, so that V_A data may be used reasonably for discussion of the plasticity mechanisms.

RESULTS AND DISCUSSION

Thermal Behavior and Structure

The quenched and annealed films are thoroughly isotropic and relaxed, as judged from the absence

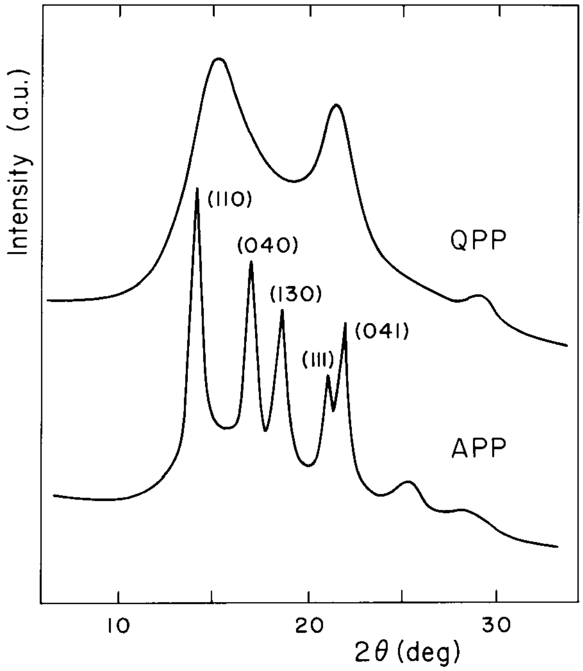

Figure 1 WAXS intensity profiles of QPP and APP films.

of preferred orientation on the WAXS patterns, as well as no measurable shrinkage upon heating above the melting point.

The WAXS intensity profiles of isotropic QPP and APP are reported in Figure 1. The WAXS profile of QPP is relevant to the so-called smectic state,[19–25] while that of APP reveals a clear cut monoclinic crystalline structure. The smectic form of PP, otherwise the mesomorphic state, consists of parallel chains having a high degree of order in their longitudinal arrangement but lacking crystallographic register in their lateral packing.[19,21,23,24] Besides the helix conformation of the crystal stems is preserved, as revealed by infrared (IR) spectroscopy.[19,22] The smectic form that is commonly obtained by quenching thin films from the molten state down to temperatures in the range of 0–40°C can be considered as a "frozen in" intermediate state of order in the crystallization pathway.[21] This is a consequence of the fast cooling, which prematurely hinders the molecular motions necessary for the reorganization process. It is worth noticing that in this scheme, the molecular reorganization looks more like a spinodal decomposition rather than a nucleation and growth process.

The differential scanning calorimetry (DSC) curves of Figure 2 show a single melting endotherm for APP with a peak temperature of 167°C that corroborates the monoclinic structure. A crystal weight fraction $X_c = 0.57 \pm 0.02$ can be determined, assuming a melting enthalpy of 184 J g for a perfect PP crystal. In contrast, QPP displays an endotherm at about 70°C followed by an exotherm with a peak temperature close to 110°C that are characteristic of a reorganization process of the smectic phase into the monoclinic form.[20,23,25] This latter melts at higher temperature, as revealed by the sharp endotherm at about 165°C.

Viscoelastic Behavior

The variations with temperature of the storage modulus E' and loss factor tan δ are reported in Figure 3 for the two kinds of films. The two $E'(T)$ curves are quite similar below the β relaxation at about 10°C, that is, the glass transition of isotactic polypropylene at 1 Hz. Above 10°C, E' drops with increasing temperature as a result of the gradual activation of the molecular mobilities in the crystalline phase, the so-called α relaxation.[26] However, QPP displays a steeper E' drop than APP due to weaker elastic interactions in the smectic phase than in the monoclinic phase. This is supported by the higher tan δ level of QPP between 10 and 60°C that indicates greater energy absorption due to more intense molecular

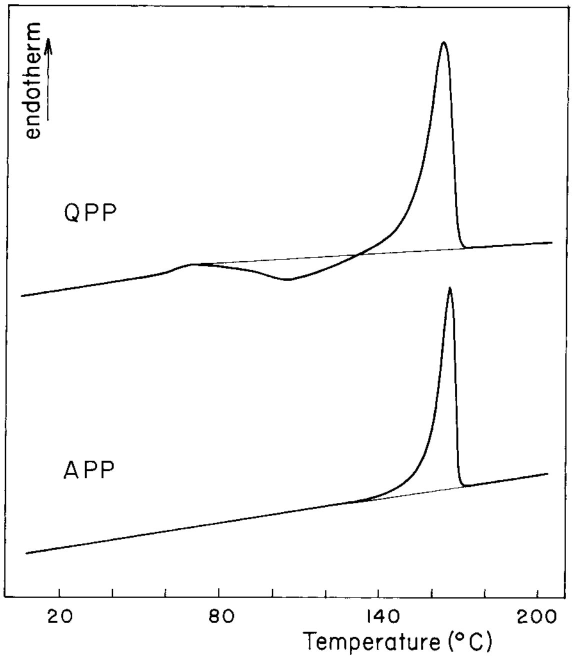

Figure 2 DSC traces of QPP and APP films.

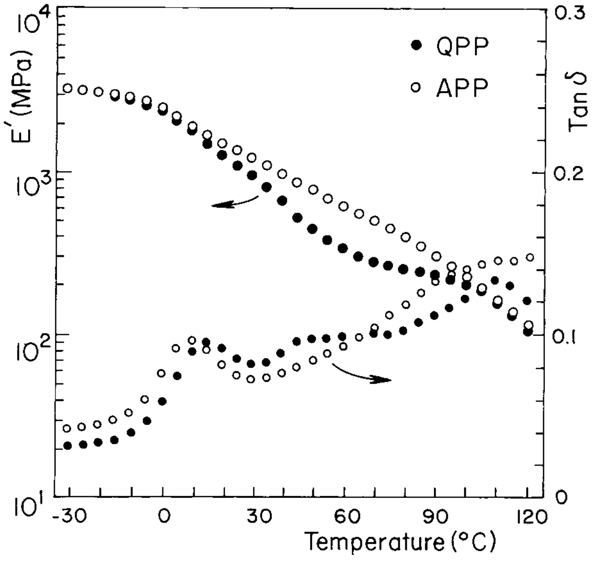

Figure 3 Storage modulus and loss factor for QPP and APP films.

mobility. There is comparatively minor difference of molecular mobility in the amorphous component of the two films, as judged from the departure of only 5° between the β peaks.

In the temperature range 70–110°C, the drop of QPP modulus is less pronounced than that of APP, so that the two curves merge above 110°C. This is relevant to the transformation of the smectic phase of QPP into the stable monoclinic form in the meantime of the experiment thanks to the increasing activation of the molecular motions in the ordered phase.

The tan δ peak magnitude of the β relaxation is about the same for the two kinds of materials, indicating that the amount of amorphous phase is not significantly affected by the annealing treatment, which just turns the mesomorphic domains into monoclinic crystals. This allows us to analyze the influence of the intrinsic properties of the ordered component, namely, smectic or monoclinic, on the mechanical behavior of the films, disregarding its concentration.

It is to be noticed that the temperature at which the reorganization in the crystalline phase begins in QPP on the mechanical standpoint, that is, 70°C, is precisely the temperature at which the reorganization proceeds on a thermodynamic standpoint (Fig. 2). This is a piece of evidence that the occurrence of the smectic state is directly connected with the freezing of some molecular mobilities, which affects the kinetic part of the crystallization process under fast cooling conditions. An analogous phenomenon has been observed for ethylene—vinyl–alcohol copolymers,[27] which display a mesomorphic state upon quenching. In this case, both thermal analysis and X-ray diffraction (XRD) indicated a prompt recovery of the crystalline stable form by annealing above the peak temperature of the crystalline mechanical relaxation.

Tensile Drawing Behavior

The nominal stress–strain curves of Figure 4 show a yield stress depression for QPP compared to APP. This often reported phenomenon[28–32] is a consequence of the lower molecular cohesion of the smectic phase compared to the monoclinic phase. Considering that the mechanical behavior of the amorphous phase is unchanged between the two samples, as judged from the minor change in the β relaxation temperature, the above observation reveals the major role of the ordered phase in the plastic behavior. Beyond the draw plateau corresponding to the propagation of a plastic instability (that is, necking) over the whole length of the sample, strain-hardening occurs as a result of chain unfolding and orientation involving the so-called fibrillar transformation. The strain-hardening rate of QPP in the post-yield domain is stronger than that of APP so that the gap between the two curves is gradually reduced, and the two samples finally break at roughly equivalent stress. This finding is relevant to either a structural hardening of QPP due to a gradual smectic-

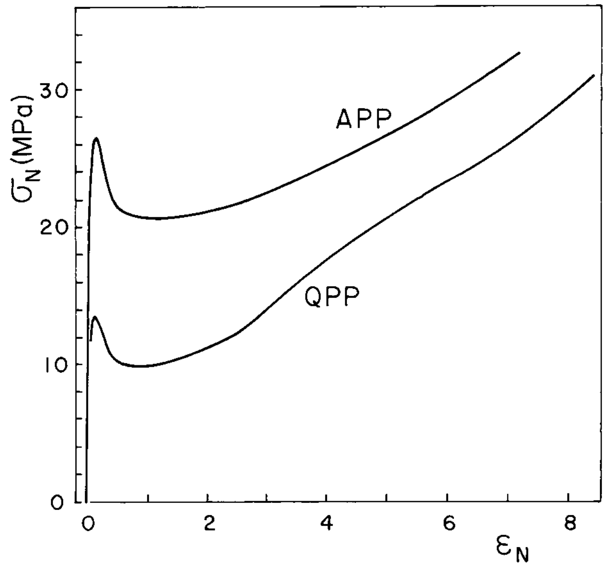

Figure 4 Nominal stress–strain curves for QPP and APP films at 40°C (strain rate $\dot{\varepsilon} = 1.05 \times 10^{-2}$ s^{-1}).

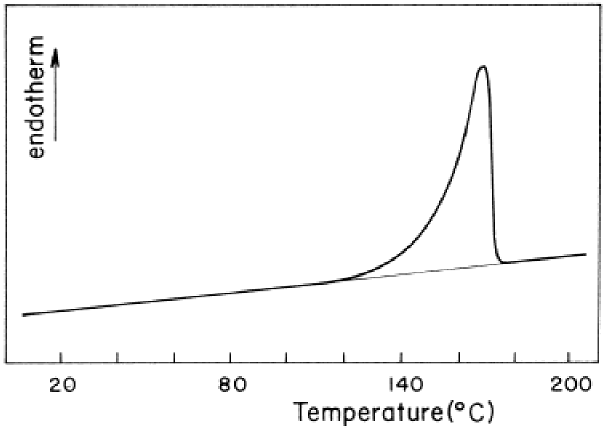

Figure 5 DSC traces of a sample from a QPP film drawn at T_d = 40°C up to the strain $\varepsilon \approx 2.5$ (strain rate $\dot{\varepsilon} = 1.05 \times 10^{-2}$ s^{-1}).

to-monoclinic (s → m) phase change or to a structural softening of APP due to a monoclinic-to-smectic (m → s) phase change.

Strain-Induced Phase Change

The structural change suggested above from the analysis of the tensile drawing curves has been investigated by DSC and WAXS measurements. The DSC curve of a QPP sample drawn at 40°C up to $\varepsilon \approx 2.5$, at the strain rate $\dot{\varepsilon} = 1.05 \times 10^{-2}$ s^{-1}, is reported in Figure 5. The absence of the exotherm peak associated with the reorganization of the smectic phase into monoclinic crystals during the heating scan indicates that most of the transformation has already occurred during the drawing stage. The melting endotherm is however broader than that of the isotropic APP (Fig. 2) revealing a large distribution of crystal defect concentration and size. The WAXS pattern of the same sample, as in Figure 5, is reported in Figure 6. This pattern displays the main reflections of the monoclinic structure and thoroughly support the s → m strain-induced phase change.

The equatorial WAXS intensity profile of the pattern of Figure 6 is reported in Figure 7, together with the profile from a QPP sample drawn for the same conditions, that is, at 40°C and $\varepsilon \approx 2.5$; but for a higher strain rate, $\dot{\varepsilon} = 1.05 \times 10^{-1}$ s^{-1}. The location of the major peak at $2\theta = 14°$ for the two profiles of Figure 7 is definitively relevant to the predominance of the monoclinic structure since the smectic major peak is located at $2\theta = 15°$.[10,23] The two diffraction peaks in the range $16° < 2\theta < 19°$ support the above conclusion. However, the broadness of the reflections compared to the WAXS profile of APP (Fig. 1) is in

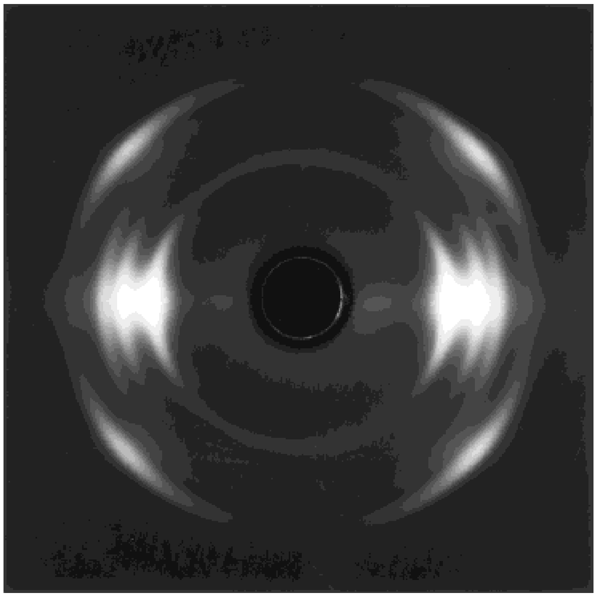

Figure 6 WAXS pattern of the same QPP drawn film as in Figure 5.

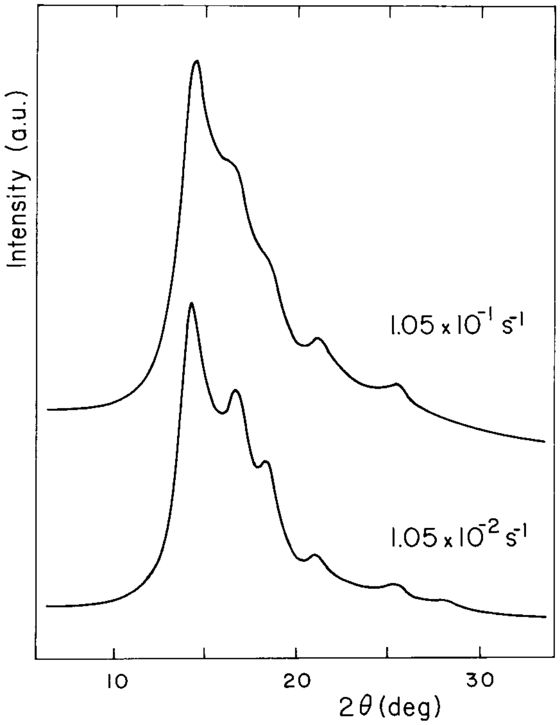

Figure 7 Equatorial WAXS intensity profiles of QPP samples drawn at T_d = 40°C up to the strain $\varepsilon \approx 2.5$ for two different strain rates, $\dot{\varepsilon} = 1.05 \times 10^{-2}$ s^{-1} and $\dot{\varepsilon} = 1.05 \times 10^{-1}$ s^{-1}.

agreement with the previously suspected presence of rather small and imperfect monoclinic crystals. Besides, some minor smectic structure may remain, but is not clearly detectable beneath the monoclinic scattering.

The very strong drop of scattered intensity in the range $20° < 2\theta < 23°$ is due to the quadrant azimuthal position of the (111) and (041) monoclinic reflections from the fiber structure (see Fig. 6).

The increasing broadness of the reflections as strain rate increases reveals the kinetic aspect of the structural reorganization. The very short time afforded to the process at high strain rate is not favorable to the achievement of great crystalline perfectness.

Figure 8 shows the equatorial WAXS intensity profiles of two QPP samples drawn at 25 and 60°C, up to the strain $\varepsilon \approx 2.5$, for the strain rate $\dot{\varepsilon} = 1.05 \times 10^{-1}$ s^{-1}. The much well-resolved monoclinic peaks observed for 60°C constitute an additional piece of evidence that the reorganization process of the metastable crystalline form into a more ordered and stable form is kinetically governed.

There are two points of view on the mechanism of phase change accompanying plastic deformation of semicrystalline polymers since both order–disorder and disorder–order transitions have been reported. In an extensive review of the phenomenon, Saraf and Porter[33] concluded that the induced ductility that is gained from an order-to-disorder transition is a route to optimize solid-state deformation. In contrast, Karger–Kocsis[34] suggested that phase transition from a less toward a more dense crystalline state may be a means for toughness upgrading.

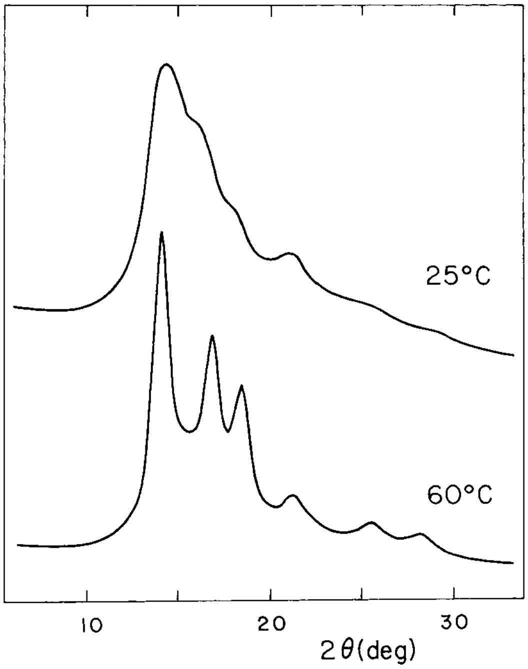

Figure 8 Equatorial WAXS intensity profiles of QPP samples drawn at T_d = 25 and 60°C up to the strain $\varepsilon \approx 2.5$ (strain rate $\dot{\varepsilon} = 1.05 \times 10^{-1}$ s^{-1}).

In the case of PP, both the s → m and the m → s transformations have been actually observed. We believe that these two opposite situations have a different driving force. On the one hand, at the scale of the microscopic plasticity event, the mechanical work brought about by the applied stress reduces the thermodynamic barrier between the metastable and stable crystals and thus helps the chains to find their way towards more stable potential energy wells during the deformation process. Besides, drawing at large strains involves strong molecular orientation that improves the kinetics of molecular rearrangement into the more stable and denser crystalline form. This is analogous to the strain-induced crystallization of quenched semicrystalline polymers, such polyethylene terephthalate,[35] that may take place at temperatures just above the glass transition for which thermal crystallization is nil. In this case, the driving force of the phase change relies on thermodynamic and kinetic factors. On the other hand, the plastic deformation of monoclinic PP is likely to proceed through a transient promotion of the smectic phase[36] that allows a lower energy-consuming pathway owing to its lower molecular cohesion. This situation has been largely discussed by Porter and Saraf for bulk PP submitted to compressive testing.[10,11,23,37] In this case, the driving force of the phase change relies on energetic grounds. A molecular mechanism of generation of the smectic phase is discussed below in relation to the mechanism of crystal slip in the special case of PP chains having a helix conformation.

Thermal Activation of Yield

The yield stress dependence on strain rate for QPP is reported in Figure 9 for various draw temperatures not exceeding 60°C in order to prevent thermal conversion of the smectic structure into monoclinic crystal. For 5 and 25°C over the whole strain rate range, as well as for 40°C in the strain rate range $\dot{\varepsilon} > 10^{-2}$ s^{-1}, the slope of the

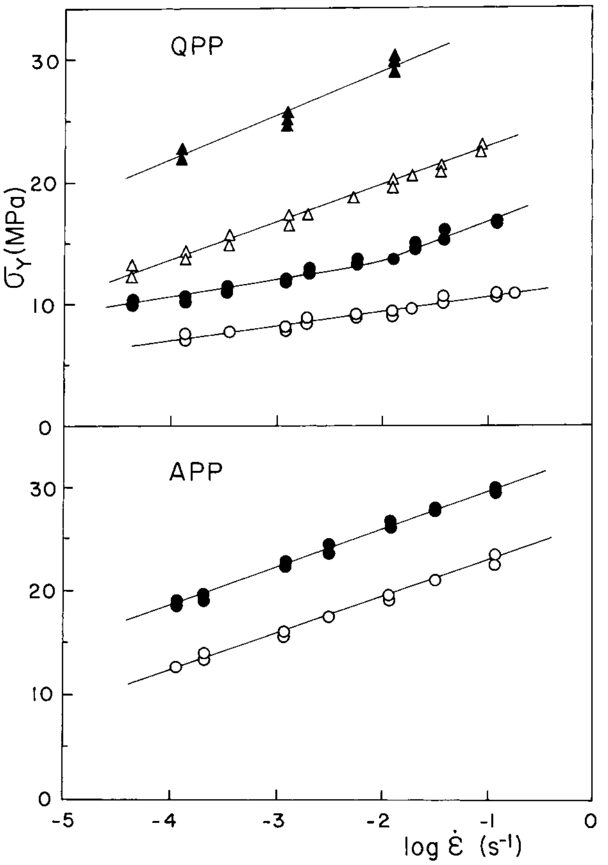

Figure 9 Yield stress σ_Y versus strain rate $\dot{\varepsilon}$ for QPP and APP at various draw temperatures: (▲) 5, (△) 25, (●) 40, and (○) 60°C.

σ_Y(Ln $\dot{\varepsilon}$) curves is about the same, indicating a common elementary process of plastic flow with an apparent activation volume of about 3.0 nm^3 [see eq. (A.4) in the Appendix]. For 40°C in the range of strain rate $\dot{\varepsilon} < 10^{-2}$ s^{-1}, and for 60°C over the whole $\dot{\varepsilon}$ range, the apparent activation volume is about 7.7 nm^3. This is indicative of a second plastic deformation regime involving a change in the structural extent of the elementary event of plastic flow (see the warning of the Activation Volume Determination and Signification Section in the Appendix), in relation to draw temperature and strain rate.

In the case of APP, yield stress measurements have been only carried out at 40 and 60°C due to the brittleness of the film at lower temperatures. At 20°C, for instance, the samples systematically broke for $\dot{\varepsilon} > 10^{-3}$ s^{-1}. From the data reported in Figure 9, the apparent activation volume at 40 and 60°C is about 3.0 nm^3, that is, a value close to that found for QPP at low temperature. This means that the elementary event of plastic deformation is the same for the two kind of materials, in the draw conditions indicated above.

The two activation volumes observed in the case of QPP are relevant to a change in the basic mechanim of plasticity. This could be ascribed to the strain-induced change of structure from smectic to monoclinic, as discussed in the preceding section. Indeed, although undetected as a permanently settled phenomenon at the yield point, the phase change might begin to take place as a transitory phenomenon at this stage of the plastic deformation, depending on T_d and $\dot{\varepsilon}$ conditions. This phase change may be accompanied by a change of activation volume since the reduced molecular cohesion in the smectic phase involves enhanced mobility and thereby allows better cooperativity, that is, a larger activation volume. However, two experimental facts argue against it. First, the larger activation volume of QPP at 60°C would suggest that the smectic form is preserved at high T_d and that the s $\rightarrow$ m transformation is more favorable at low T_d. This is contradictory to the natural trend of the smectic form to turn into the monoclinic form for temperatures above 70°C. Second, the drop of activation volume observed for $\dot{\varepsilon} > 10^{-2}$ s^{-1} in the case of QPP at 40°C cannot be attributed to the s $\rightarrow$ m structural change since increasing the strain rate at a given temperature reduces the ability for the phase change, as discussed in the preceding section.

Figure 10 shows the yield stress plot versus temperature at three different strain rates. Despite the rather reduced number of data, it clearly appears that the slope of $\sigma_Y(T)$ for APP, in the range of 40–60°C, is higher than that of QPP, in the same temperature range. However, it is close to that of QPP in the range of 5–20°C. In qualitative terms [see eq. A.6 in the Activation Volume Determination and Signification Section in the Appendix), this corroborates the conclusions made above that (1) the apparent activation volume of QPP at high temperature is about twice as large than at low temperature and that (2) the latter value is close to that for APP at high temperature. Worth noting is that, in the second case, the stress level is about the same for the two kinds of samples. This emphasizes the well-known stress dependancy of the activation volume and suggests that QPP may display the same elementary mechanism of plasticity than APP, provided that the temperature is low enough to make the yield stress increase to a comparable level.

The activation volume data from stress relaxation experiments at the yield point are reported in Figure 11 for QPP and APP. These data fit fairly well with the ones reported from the analysis of the $\sigma_Y(\text{Ln}\ \dot{\varepsilon})$ curves, despite a quite different experimental procedure of determination (see the Stress Relaxation Measurements Section in the Appendix). The new matter from Figure 11 is that the more accurate V_a data reveal an almost linear drop of the activation volume as the draw temperature decreases or the strain rate increases. This means that the mechanism of the plastic flow is not a simple one. In addition, Figure 11 shows that the V_a data of QPP at 40°C are close to those at 60°C below $\dot{\varepsilon} = 10^{-2}\ \text{s}^{-1}$ and close to those at 25°C above this strain rate value. This is relevant to a change in the plastic flow mechanism of QPP as a function of strain rate at 40°C, in agreement with the phenomenon already suspected from the σ_Y versus $\dot{\varepsilon}$ variations.

In a pioneer work concerned with bulk injection-molded PP, Roetling[38] reported a change in the variation of the yield stress with strain rate that was strongly dependent on the deformation temperature. This author proposed that the activation of molecular mobilities in the amorphous phase and the melting of the crystalline phase could account for the two deformation regimes. But it is now well known that melting is not a thermally activated process and that the steady decrease of stiffness over a large temperature range above T_g is due to the mechanical relaxation process in the crystalline phase, prior to melting. The molecular basis of this phenomenon is discussed in the next section.

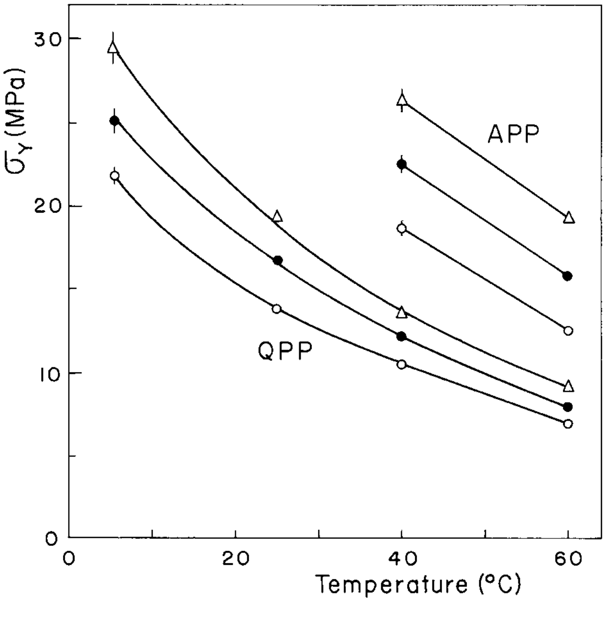

Figure 10 Yield stress, σ_Y, versus temperature for QPP and APP at three strain rates: (○) $\dot{\varepsilon} = 1.05 \times 10^{-4}\ \text{s}^{-1}$; (●) $\dot{\varepsilon} = 1.05 \times 10^{-3}\ \text{s}^{-1}$; (△) $\dot{\varepsilon} = 1.05 \times 10^{-2}\ \text{s}^{-1}$.

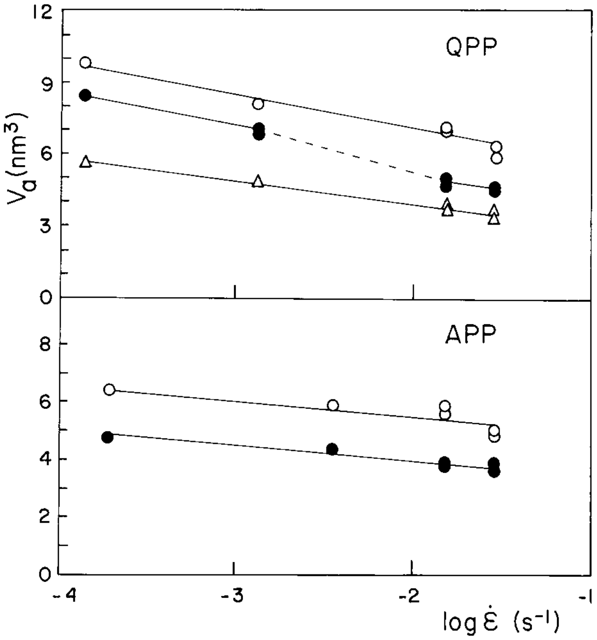

Figure 11 Activation volume V_a from stress relaxation for the plastic flow of QPP and APP as a function of strain rate $\dot{\varepsilon}$ at various draw temperatures: (△) 25, (●) 40, and (○) 60°C.

Homogeneous and Localized Crystal Slip

The photographs of Figure 12 show QPP samples drawn at 25 and 60°C up to roughly the same nominal strain $\varepsilon_N = 0.3$. For 25°C, the sample displays a sharp neck, that is, a high gradient of transverse strain along the neck shoulder. The very narrow interference fringes that appear in the regions of the neck shoulders reveal the high strain gradient in the thickness. Moreover, very coarse shear bands appear in the regions outside the neck. Both the above features are suggestive of a strong propensity for localized crystal slip at 25°C. In contrast, the sample drawn at 60°C displays diffuse neck and broader interference fringes that indicate a low strain gradient in both width and thickness in the neck shoulder. Besides, the absence of coarse shear bands, as well as the uniform birefringence outside the necked region, argue in favor of a highly active homogeneous crystal slip at 60°C.

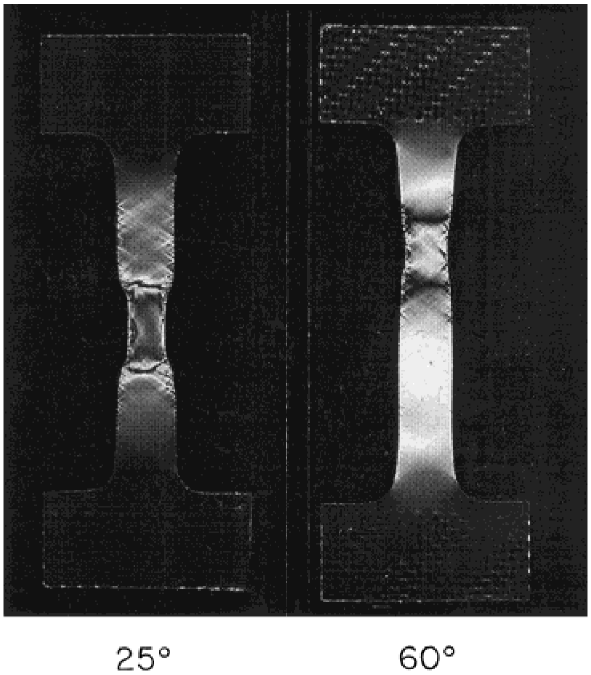

Figure 12 Scanner images of QPP sheets drawn at 25 and 60°C up to $\varepsilon_N = 0.3$, ($\dot{\varepsilon} = 1.05 \times 10^{-3}$ s^{-1}, crossed polarizers).

The above observations, together with the activation volume data, suggest that the plastic deformation of QPP obeys two different mechanisms of plasticity, depending on the draw conditions. By analogy, one may conclude that either of these two different mechanisms take place in APP and QPP at 60°C. So, alternatively to Roetling proposal, we strongly suspect a modification of the mechanisms of crystal slip that govern the plastic flow in the present case of tensile drawing above the glass transition temperature. Borrowing from our previous studies on polyethylene and related copolymers, we suggest that two mechanisms of homogeneous and localized crystal slip may operate competitively. In this instance, Yamada and Takayanagi[39] have shown the occurence of two plastic processes in oriented PP under uniaxial tension, from combined WAXS and SAXS analyses, as follows: crystal blocks may slip past each other in the fibrillar texture concurently to the uniform shear of the blocks.

Our hypothesis is that, on the one hand, above the peak temperature of the α mechanical relaxation in the crystalline phase, the molecular mobilities are high enough to allow a thermally activated nucleation and propagation of screw dislocations in response to the applied stress. The high value of the activation volume for QPP at high temperature in perfectly consistent with the above assumption. Such a mechanism, which is precursory to homogeneous or uniform crystal slip, accounts fairly well for the yielding behavior of bulk polyethylene (PE) and related copolymers,[40–42] as well as PP films.[32] On the other hand, below the peak temperature of the α mechanical relaxation, dislocations are not able to nucleate and propagate at a rate high enough to fit with the macroscopic strain rate. Then heterogeneous or localized crystal slip is likely to occur either through defective interfaces within the crystalline lamellae[41] or through the occurence of partial dislocations involving the build up of stacking faults.[43] The lower activation volume, which is relevant to a smaller extent of the elementary events of plastictity, is consistent with a reduced ability for the thermal nucleation of dislocations. Microcracks are then likely to occur.

For the ranges of temperature and strain rate investigated in this work, APP display dominant heterogeneous slip, as judged from the low activation volume. In contrast, the change of activation volume that occurs in QPP either on decreasing strain rate or on increasing temperature (see the preceding section) is relevant to a change in the crystal slip mechanism, thanks to the lower molecular cohesion in the smectic structure of QPP as compared to the monoclinic APP.

Yamada and Takayanagi[39] have reported experimental estimations of the critical shear stress (CSS) for the uniform shear lower than that of the crystal block slip, whatever the draw temperature between 40° and 130°C. This seems contradictory with our conclusion that heterogeneous slip is easier than homogeneous slip in monoclinic PP below 60°C. In fact, the fibrillar texture of the preoriented sample studied by Yamada and Takayanagi is suspected to induce a strong modification of the CSS of the two slip processes compared to isotropic PP because of the partially unfolded chain topology. Shinozaki and Groves[44] have reported combined WAXS and SAXS analyses of oriented PP and PE at room temperature that corroborate the predominence of homogeneous slip but that point out the marked trend of PP for necking and voiding notably when the lamellae make angles greater than 45° with respect to the stress axis. In final support to our statement, the study by Cerra et al.[45] of plastically deformed PP single crystals shows that only the crystal block slip is active at room temperature. According to the latter authors, this contrasts with the plastic behavior of PE single crystals, which actually display chain tilt, that is, uniform shear, in addition to block sliding.

Helix Chain Motion and Screw Dislocation Slip

The mechanism of the α mechanical relaxation that should be responsible for the nucleation and propagation of dislocations is not so simple as the one previously proposed for PE.[42] The 180° chain twist of the stems having a planar zig-zag conformation in the PE orthorhombic crystal lattice involves a shortening of the stem length equal to one C—C bond, that is, half the c crystallographic parameter. The migration of such a conformational defect through the whole length of the stem results in an overall 180° rotation and $c/2$ translation of the stem, which turns again in crystallographic register. Thanks to the regular generation of such chain defects in the neighbor stems of the same crystallographic plane, a crystalline defect of the screw dislocation type builds up and propagates. Unfortunately, the nature of the molecular motions in the crystalline phase of PP has not been clearly identified. From solid-state nuclear magnetic resonance (NMR) spectroscopy, Spiess et al. proposed a threefold rotational jump of the PP chains[46] analoguous to the twofold rotational jump of the PE chains,[47] presumably accompanied with a $c/3$ translation parallel to the chain axis. However, these authors did not mention the localized character of such processes with regard to the stem length. The well-known invariance of the α relaxation activation energy as a function of crystal thickness argues against the motion of the whole stem. This has been clearly established in the case of PE, for which 180° chain twist defects spanning about 12 methylene units are allowed to move smoothly along the chain stem. In the case of PP, Syi and Mansfield have proposed a soliton approach involving localized rotation–translation jumps operating over a shorter distance than the crystal thickness.[48]

Borrowing from Boyd's guideline for the molecular mechanisms of crystalline relaxations,[49] one may expect the occurence of mobile localized defects in the helical conformation of PP. Migration of such a defect along the chain stem results in a translation of the chain. Several kinds of conformational defects can be devised from the various helical conformations theoretically predicted for backbone-saturated polymer chains.[50] The $(TG)_3$ triple trans-gauche conformational sequence characteristic of the stable 3/1 helix of crystalline isotactic PP is contracted by about 15% compared to the all-trans conformation of PE, so that either compressive or extensive defects may occur. For instance, a compressive strain is devised in Figure 13 owing to a sequence of four monomer units in gauche conformations corresponding to a 2/1 helix chain portion within a 3/1 helix [Fig. 13(b)] compared to three monomer units in trans-gauche conformation [Fig. 13(a)]. This conformational defect that brings about an additional monomer unit within the helix pitch involves a 120° twist and a $c/3$ compression of the chain. The thermally activated nucleation and motion of

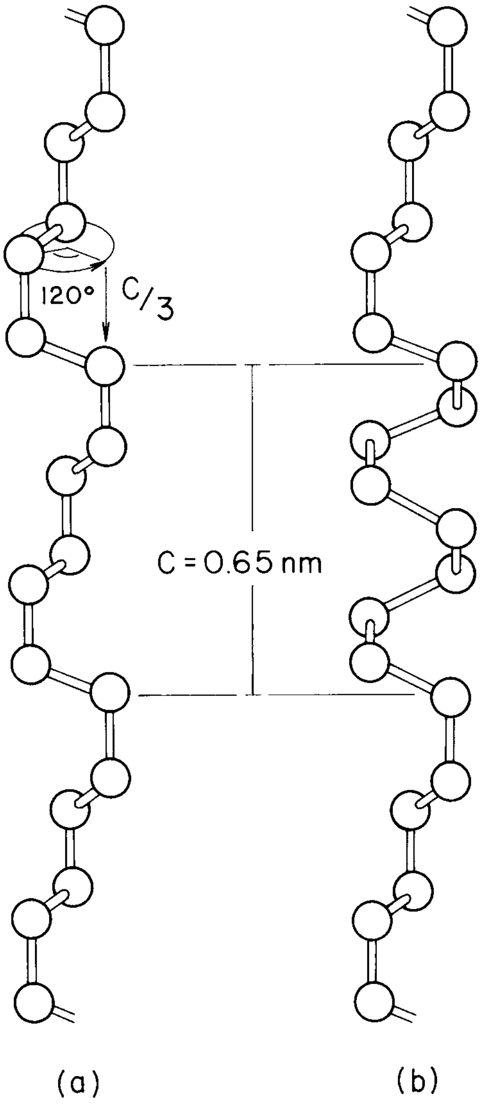

Figure 13 Polypropylene chain conformations: (a) stable 3/1 helix in $(TG)_3$ conformation; (b) defective helix with a gauche link sequence involving 120° twist and $c/3$ compressive strain.

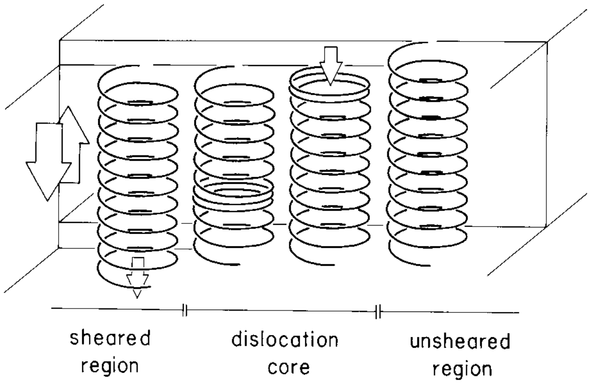

Figure 14 Molecular model of the helix chain motion for the glide of a screw dislocation along a sheared interface.

such a defect along the chain results in an overall 120° rotation and $c/3$ translation of the stem.

Figure 14 shows a schematic drawing of a local compressive strain within a few turns of a helix chain, that is, a local shortening of the helix pitch. In a similar manner as proposed for PE, a defect in a crystalline stem is initiated from one of the fold surfaces of the crystal, thanks to the resolved shear stress acting on this crystal. Then it propagates along the chain in a wormlike motion, and finally exits from the crystal at the opposite fold surface. The occurence of such a process, successively from stem to stem in a given slip plane, results in the generation and propagation of a screw dislocation.

Structural Implication of Conformational Defects

At temperatures below the peak temperature of the α crystalline relaxation, that is, when the migration of conformational defects along the chain axis is severely restricted due to kinetic factors, screw dislocations cannot be generated at a rate high enough to fit the macroscopic strain rate. Then localized slip is able to substitute homogeneous slip through the build up of stacking faults, owing to either crystal slip without chain rotation or partial rotation and translation.

This change of mechanism of plasticity, in relation to the kinetic aspect of dislocation nucleation and propagation, will be discussed in a future article. But some comments already deserve to be made regarding the conformational aspect of the problem. Indeed, it has been emphasized above that the conformational defect in the stable $(TG)_3$ conformation of the PP helix chain that allows the step-by-step translation of the chain along its own axis is a defective region with no longer crystallographic register so when the temperature is below the crystalline relaxation, frozen in conformational defects are likely to remain in the dislocations wake. A misfit may settle over large distances between the moving chains and the surrounding chains since the former ones are liable to encounter the potential energy wells of the metastable smectic structure. The growing concentration of such crystallographic defects with the increase of plastic strain is likely to develop local smectic-like chain arrangements. These plasticity defects are a possible origin for the partial strain-induced m → s transition in PP below 70°C that has been discussed previously. This is consistent with the conclusion by Saraf[11] that the smectic phase results from the chain unraveling in concert with the activation of crystal slip process.

CONCLUSION

The study of the tensile yielding of PP films shows that the metastable smectic form induced by quenching is more ductile than the stable monoclinic form due to reduced intermolecular cohesion. For strains $\varepsilon \geq 3$, a strain-induced transformation of the smectic form into the monoclinic form occurs. The stress-induced chain defects improve the molecular mobility, which reduces the thermodynamic barrier between the two forms. Chain orientation also contributes to the reorganization process through the improvement of its kinetics.

Homogeneous and localized crystal slip are proposed to account for the two plastic deformation regimes observed in the case of QPP. The reason lies in the mobility of the conformational chain defects that are necessary for generation and motion of crystal dislocations. Homogeneous crystal slip takes place when homogeneous nucleation and propagation of screw dislocations are fast enough to provide a local strain rate consistent with the macroscopic applied strain rate. Only localized slip seems to occur in APP, for $T \leq 60°C$. The stronger interactions in the monoclinic structure compared to the smectic structure is responsible for a reduced mobility of the chain defects in the ordered phase of APP.

It is suggested that the molecular mechanism of chain relaxation consists of a local compressive strain of the helix chain that moves in a wormlike motion along the chain axis. The particularly large c crystallographic parameter of the monoclinic unit cell entails that the chain will be out of crystallographic register over a long distance. During its progression through the crystal thickness, the defective chain portion may occasionally encouter the metastable potential energy wells of the smectic form so that this phase may be strain-induced from the monoclinic phase for temperatures below the α crystalline relaxation.

The authors thank PECHINEY for financial support to this work and for the grant of a doctorate research fellowship to E. Staniek.

APPENDIX

Activation Volume Determination and Signification

The Eyring equation for plastic flow writes

$$\dot{\varepsilon} = \dot{\varepsilon}_0 \exp - \left(\frac{\Delta G(\sigma, T)}{kT} \right)_{\varepsilon, T} \qquad \text{(A.1)}$$

where $\dot{\varepsilon}$ is the plastic strain rate, $\Delta G(\sigma, T)$ is the activation energy, T is the absolute temperature, k is the Boltzman constant, ε is the plastic strain, and σ is the stress. The preexponential factor often obeys a stress power law,[18]

$$\dot{\varepsilon}_0 = K\sigma^m \qquad \text{(A.2)}$$

where K is a constant, and m is the stress intensity factor, which lies in the range of 2–3. Considering that the applied stress at yield helps to reduce the energy barrier to thermal flutuations, $\Delta G_0(T)$, then

$$\Delta G(\sigma, T) = \Delta G_0(T) - V_0\sigma \qquad \text{(A.3)}$$

with V_0 being the true activation volume. This latter is related to the strain rate sensitivity through the following relation:

$$V_0 + kT\left(\frac{\partial \text{ Ln } \dot{\varepsilon}_0}{\partial \sigma} \right)_{\varepsilon, T} = kT\left(\frac{\partial \text{ Ln } \dot{\varepsilon}}{\partial \sigma} \right)_{\varepsilon, T} = V_a \qquad \text{(A.4)}$$

The apparent activation volume V_a that can be obtained from the experimental slope of the yield stress versus Ln $\dot{\varepsilon}$ plot is related to the true activation volume thanks to an additional stress-dependent term.

$$V_a = V_0 + mkT/\sigma \qquad \text{(A.5)}$$

At the lower stress level of the present investigation, that is, about 10 MPa, for which V_a has the higher value of 7.7 nm^3, the larger value of the stress-dependent term can be estimated to 1.2 nm^3. For the higher stress level, that is, 30 MPa, for which V_a has the lower value of 3.0 nm^3, this additional term drops to about 0.4 nm^3. For the present study, the apparent activation volume V_a, therefore, gives a fair estimation of the true activation volume V_0 since the error does not exceed 15%.

The apparent activation volume may also be assessed, using eq. (1), from the temperature dependancy of the stress at yield point derived, as follows:

$$V_a = k \text{ Ln}(\dot{\varepsilon}/\dot{\varepsilon}_0) \left(\frac{\partial T}{\partial \sigma} \right)_{\varepsilon, \dot{\varepsilon}} \qquad \text{(A.6)}$$

Stress Relaxation Measurements

Determinations of the apparent activation volume V_a can be carried out through stress relaxation measurements as a function of time t at a stress level close to the yield point.[17] The stress drop $\Delta\sigma(t)$ is given by

$$\Delta\sigma(t) = \frac{kT}{V_a} \text{Ln}\left(\frac{t}{C} + 1 \right) \qquad \text{(A.7)}$$

where $C = kT/MV_a\dot{\varepsilon}$ is an integration constant, with M being the modulus of the material, and $\dot{\varepsilon}$ is the plastic strain rate.

REFERENCES

1. Peterlin, A.; Balta-Calleja, F. J. J Appl Phys 1969, 40, 4238.
2. Balta-Calleja, F. J.; Peterlin, A. J Macromol Sci, Phys 1970, B4, 519.
3. Sakaoku, K.; Peterlin, A. J Polym Sci, Polym Phys 1971, 9, 895.
4. Samuels, R. J. Polym Eng Sci 1976, 16, 1741.
5. De Vries, A. J. Polym Eng Sci 1983, 23, 241.
6. Pan, S. J.; Brown, H. R.; Hiltner, A.; Baer, E. Polym Eng Sci 1986, 26, 997.
7. Karakan, I.; Taraiya, A. K.; Bower, D. I.; Ward, I. M. Polymer 1993, 34, 2691.
8. Dahoun, A.; G'Sell, C.; Favier, V.; Hiver, J. M.; Philippe, M. J.; Canova, G. R. Polym Eng Sci 1997, 37, 1702.

9. Aboulfaraj, M.; G'Sell, C.; Ulrich, B.; Dahoun, A. Polymer 1995, 36, 713.
10. Saraf, R.; Porter, R. S. Polym Eng Sci 1988, 28, 842.
11. Saraf, R. F. Polymer 1994, 35, 1359.
12. Bartczak, Z.; Argon, A. S.; Cohen, R. E. Macromolecules 1992, 25, 5036.
13. Bartczak, Z.; Argon, A. S.; Cohen, R. E. Polymer 1994, 35, 3427.
14. G'sell, C.; Dahoun, A. Mater Sci Eng 1994, A175, 183.
15. Galeski, A.; Argon, A. S.; Cohen, R. E. Macromolecules 1991, 24, 3953.
16. Lin, L.; Argon, A. S. Macromolecules 1994, 27, 6903.
17. Porzucek, K.; Coulon, G.; Lefebvre, J. M.; Escaig, B. J Mater Sci 1989, 24, 2533.
18. Escaig, B. Ann Phys 1978, 3, 207.
19. Miller, R. L. Polymer 1961, 2, 185.
20. Farrow, G. J Appl Polym Sci 1965, 9, 1227.
21. Wunderlich, B.; Grebowicz, J. Adv Polym Sci 1984, 60/61, 1.
22. Hendra, P. J.; Vile, J.; Willis, H. A.; Zichy, V.; Cudby, M. E. A. Polymer 1984, 85, 785.
23. Saraf, R.; Porter, R. S. Mol Cryst Liq Cryst Lett 1985, 2, 85.
24. Corradini, P.; Petraccone, V.; de Rosa, C.; Guerra, G. Macromolecules 1986, 19, 2699.
25. Vittoria, V. J Macromol Sci, Phys 1989, B28, 489.
26. Jourdan, C.; Cavaille, J. Y.; Perez, J. J Polym Sci, Polym Phys Ed 1989, 27, 2361.
27. Penel, L.; Djezzar, K.; Lefebvre, J.-M.; Séguéla, R.; Fontaine, H. Polymer 1998, 39, 4279.
28. Gezovich, D. M.; Geil, P. H. Polym Eng Sci 1968, 8, 210.
29. Wills, A. J.; Capaccio, G.; Ward, I. M. J Polym Sci, Polym Phys 1980, 18, 493.
30. Rolando, R. J.; Krueger, W. L.; Morris, H. W. Polym Mater Sci Eng 1985, 52, 76.
31. Alberola, N.; Fugier, M.; Petit, D.; Fillon, B. J Mater Sci 1995, 30, 860.
32. O'Kane, W. J.; Young, R. J.; Ryan, A. J. J Macromol Sci 1995, B34, 427.
33. Saraf, R.; Porter, R. S. J Polym Sci, Polym Phys 1988, 26, 1049.
34. Karger-Kocsis, J. Polym Eng Sci 1996, 36, 203.
35. le Bourvellec, G.; Monnerie, L.; Jarry, J. P. Polymer 1987, 28, 1712.
36. Grebowicz, J.; Lau, S.-F.; Wunderlich, B. J Polym Sci, Polym Symp 1984, 71, 19.
37. Osawa, S.; Porter, R. S. Polymer 1994, 35, 545.
38. Roetling, J. A. Polymer 1966, 7, 303.
39. Yamada, K.; Takayanagi, M. J Appl Polym Sci 1979, 24, 781.
40. Darras, O.; Séguéla, R. J Polym Sci, Polym Phys 1993, 31, 759.
41. Gaucher-Miri, V.; Séguéla, R. Macromolecules 1997, 30, 1158.
42. Séguéla, R.; Gaucher-Miri, V.; Elkoun, S. J Mater Sci 1998, 33, 1273.
43. Séguéla, R.; Elkoun, S.; Gaucher-Miri, V. J Mater Sci 1998, 33, 1801.
44. Shinozaki, D. M.; Groves, G. W. J Mater Sci 1973, 8, 1012.
45. Cerra, P.; Morrow, D. R.; Sauer, J. A. J Macromol Sci 1969, B3, 33.
46. Schaefer, D.; Spiess, H. W.; Suter, U. W.; Fleming, W. W. Macromolecules 1990, 23, 3431.
47. Schmidt-Rohr, K.; Spiess, H. W. Macromolecules 1991, 24, 5288.
48. Syi, J. L.; Mansfield, M. L. Polymer 1988, 29, 987.
49. Boyd, R. H. Polymer 1985, 26, 1123.
50. Tadokoro, H. Structure of Crystalline Polymers; Wiley-Interscience: New York, 1979; p 13.